Scaling relations of the time-dependent Dirac equation describing multiphoton ionization of hydrogenlike ions

I. V. Ivanova,[1,2,*] V. M. Shabaev,[1] Dmitry A. Telnov,[1] and Alejandro Saenz[3]

[1]*Department of Physics, St. Petersburg State University, 7-9 Universitetskaya Naberezhnaya, 199034 St. Petersburg, Russia*
[2]*NRC "Kurchatov Institute," 1 Akademika Kurchatova Pl., 123182 Moscow, Russia*
[3]*Institut für Physik, Humboldt-Universität zu Berlin, Newtonstraße 15, 12489 Berlin, Germany*

(Received 17 October 2018; published 3 December 2018)

Approximate scaling laws with respect to the nuclear charge are introduced for the time-dependent Dirac equation describing hydrogenlike ions subject to laser fields within the dipole approximation. In particular, scaling relations with respect to the laser wavelengths and peak intensities are discussed. The validity of the scaling relations is investigated for two-, three-, four-, and five-photon ionization of hydrogenlike ions with nuclear charges ranging from $Z = 1$ to 92 by solving the corresponding time-dependent Dirac equations adopting the properly scaled laser parameters. Good agreement is found and thus the approximate scaling relations are shown to capture the dominant effect of the response of highly charged ions to intense laser fields compared to that of atomic hydrogen. On the other hand, the remaining differences are shown to allow for the identification and quantification of additional, purely relativistic effects in light-matter interaction.

DOI: 10.1103/PhysRevA.98.063402

I. INTRODUCTION

The development of light sources with extreme peak intensities remains an active field of research and technology. The extreme light infrastructure (ELI) [1,2] strives for laser peak intensities of up to 10^{24} W/cm^2 and free-electron lasers, such as the X-ray Free Electron Laser (XFEL) [3] at Hamburg and the Linear Coherent Light Source (LCLS) [4] at Stanford, are expected to produce fields with peak intensities of up to 10^{25} W/cm^2 and wavelengths down to 0.05 nm. Especially in combination with mobile electron-beam ion traps (EBIT), these light sources can investigate the interaction of highly charged ions with extremely intense light. Moreover, the High-Intensity Laser Ion-Trap Experiment (HILITE) is under construction at GSI, Darmstadt. The goal of this experiment is to study the interaction of atoms and ions confined in a Penning trap and exposed to very intense laser light [5,6]. It is planned to carry out experiments on ionization and excitation of highly charged ions (up to uranium) exposed to strong laser pulses in the framework of the Stored Particles Atomic Physics Research Collaboration (SPARC) project.

Significant advances in light-source technology have stimulated a considerable interest in the theoretical investigations of heavy one-electron ions exposed to electromagnetic radiation with extremely high frequencies and intensities. Clearly, a fully relativistic treatment of the ion-laser interaction is required for the correct theoretical description of the experiments with highly charged ions and extremely intense laser fields. Many relativistic approaches for the description of the ion-laser interaction have been suggested recently [7–19]. They include simplified models based on the Coulomb-corrected relativistic strong-field approximation (SFA) [12,13], as well as various full-dimensional solutions of the time-dependent Dirac equation (TDDE) [7–11,14–19]. Some studies [8,10,11,14] treat the interaction of the ion with the electromagnetic field within the so-called dipole approximation where the spatial dependence of the vector potential is neglected. The dipole approximation is a traditional approach for the infrared, visible, and ultraviolet light; in this frequency range it is usually well justified, since the wavelength by far exceeds the size of the ion. This is not necessarily the case for the hard x-ray radiation, and several attempts have been made to go beyond the dipole approximation, taking into account the spatial properties of the laser pulse [7,9,15–19]. If the photon energy and/or peak intensity of the laser pulse increases, the nondipole effects become more and more important, eventually making the theoretical description beyond the dipole approximation mandatory. However, for the experiments which will be carried out in the nearest future, a wide range of energies and intensities still exists where the dipole approximation is expected to be nevertheless reasonably well fulfilled.

Due to its relative simplicity, the hydrogen atom plays an important role in exploration of the light-matter interaction. In the nonrelativistic case, the corresponding time-dependent Schrödinger equation (TDSE) can, at least within the dipole approximation, be solved efficiently for most of the practically relevant laser pulses. The results derived or obtained for atomic hydrogen may then be used to approximately predict the behavior of more complex atoms or even molecules in intense laser fields. For example, the scaling properties of the generalized multiphoton ionization cross sections with respect to the nuclear charge were studied in [20] in order to provide semiquantitative predictions for the strong-field behavior of complex atoms based on the theoretical results obtained for hydrogen. In [21], it was shown that for hydrogenlike systems like positronium or highly charged one-electron ions there

*irina.ivanova@spbu.ru

exist *exact* analytical scaling relations within the dipole approximation. In this case, the response of such systems to one laser pulse can be mapped onto the response of the hydrogen atom to a laser pulse with correspondingly scaled parameters.

For experimentalists, the scaling relations are helpful in planning experiments. In fact, one of the main problems in experiments with light sources of very extreme peak intensities is the proper light-source characterization, including the determination of the peak intensity (see, for example, [22–25]). On the basis of validated scaling relations, highly charged ions may be used as a calibration tool, since one could compare the experimental results obtained when exposing an ion with a small nuclear charge to a well-characterized reference laser pulse that has a comparatively low intensity with those obtained for exposing a highly charged ion to the high-intensity laser pulse that should be characterized.

However, for the relativistic TDDE describing atomic hydrogen exposed to an intense laser field, no *exact* scaling relations could be found. Nonetheless, in [10] an *approximate* scaling law was proposed that matches the nonrelativistic solutions of the TDSE and the relativistic solutions of the TDDE for a one-electron atomic ion. In the TDSE, an auxiliary (scaled) nuclear charge is used that corrects the nonrelativistic ionization potential to match the relativistic one. As shown in [10], this gives good agreement between the TDSE results obtained with the scaled nuclear charge and the TDDE calculation, with the true nuclear charge for multiphoton ionization with the number of absorbed photons ranging from 2 to 5.

In the present work, we suggest an approximate scaling relation for the TDDE with respect to variation of the nuclear charge. Based on the scaling laws of [10,21], we derive this relation for the hydrogenlike ions exposed to intense laser fields. The validity of our scaling law is demonstrated by calculations of the ionization yields of several hydrogenlike ions subject to very short and intense laser pulses. For this purpose, we solve the TDDE numerically using the dipole approximation and length gauge. We report the results by adopting the TDDE scaling relations for the ions with the nuclear charges from 1 to 92 in the multiphoton ionization processes with absorption of two, three, four, and five photons, for a wide (2 orders of magnitude) range of laser peak intensities. By comparing the TDDE results for one-electron ions with different nuclear charges, the validity of the scaling relation can be tested. At the same time, the remaining deviations, which have essentially relativistic nature, can be quantified and their functional behavior can be analyzed. This is of interest both for understanding the relevance and magnitude of various relativistic effects in light-matter interaction, but also in order to allow for at least some approximate prediction about the behavior of highly charged one-electron atoms (or even more complex systems) in very intense laser fields.

The paper is organized as follows. In Sec. II a simple scaling law of the TDDE is suggested and the method of solving the TDDE is described. Applicability of the scaling relation in multiphoton ionization is tested in Sec. III B for the wavelength range corresponding to absorption of two to five photons. In Sec. III C, the validity of this relation is discussed with respect to the laser peak intensity. Our scaling relation captures the dominant relativistic effects in multiphoton ionization. However, some smaller relativistic corrections are not taken into account and cause a deviation of the result predicted by the scaling relation and that obtained by numerical solution of the TDDE. Such fine relativistic effects are investigated in Sec. III D. Section IV contains conclusion remarks. Atomic units (a.u.) $\hbar = e = m_e = 1$ are used throughout the paper unless specified otherwise.

II. THEORY AND COMPUTATIONAL METHOD

A. Scaling of the TDDE with respect to the nuclear charge number

It is well known that the TDSE for Coulomb systems interacting with external electromagnetic fields in the dipole approximation satisfies the exact scaling laws with respect to the nuclear charge and the reduced mass (see [21]). For example, the proper scaling of the spatial and the time variables in the equation itself as well as in the pulse parameters converts the TDSE for the hydrogenlike ion with the nuclear charge Z into the TDSE for the hydrogen atom ($Z = 1$). We shall refer to these scaling laws as the nonrelativistic scaling relations. They can be briefly summarized as

$$\begin{aligned} r &\to r/Z, \\ t &\to t/Z^2, \\ \omega &\to \omega Z^2 (\text{implying } \lambda \to \lambda Z^{-2}), \\ F_0 &\to F_0 Z^3 (\text{implying } I \to I Z^6), \end{aligned} \tag{1}$$

where r is the radial position coordinate, t is the time, ω is the laser frequency, λ is the wavelength, F_0 is the peak electric field strength, and I is the laser peak intensity. If the dynamics of the hydrogenlike ion in the laser field is described by the TDDE, the same scaling laws do not apply, even if the dipole approximation is used. Discrepancies between the results of the calculations with the original TDDE and those subject to the nonrelativistic scaling relations are shown and discussed below in Sec. III A.

In general, deviations of the results obtained with the TDDE from the corresponding results obtained with the TDSE for the same system can be attributed to relativistic effects. In Ref. [10], it was shown that the main relativistic effect is due to the shift of the ionization potential. A scaling relation was proposed to account for this effect (see Eq. (27) in [10]). This relation suggests a scaled nuclear charge Z' related to the true (physical) charge Z *via*

$$Z' = \sqrt{2c^2(1 - \sqrt{1 - Z^2/c^2})}. \tag{2}$$

As was shown for $Z = 50$ in [10], calculations of multiphoton ionization using the TDSE with the scaled charge Z' are in good agreement with the calculations using the TDDE and the true charge Z. At least the scaling relation (2) works well in the almost perturbative ionization regime considered in [10], confirming that the dominant relativistic effect in this case is the modification of the ionization potential. Other possible relativistic effects appeared to be negligibly small.

In this work, we suggest an *approximate* scaling law for the TDDE describing hydrogenlike ions in laser fields. The approximate TDDE scaling relation implies that the behavior of the hydrogenlike ion with the nuclear charge Z exposed to a laser pulse with the carrier wavelength $\lambda(=2\pi c/\omega)$ and peak intensity $I(=cF_0^2/8\pi)$ is *almost* the same as that of the ion with the nuclear charge $\tilde{Z}$ exposed to a pulse with a carrier wavelength $\tilde{\lambda}$ and peak intensity $\tilde{I}$. Based on the previous results [10,21], we derive the scaling relations between λ and $\tilde{\lambda}$, I and $\tilde{I}$ valid for a wide range of the nuclear charges. The principal idea is to combine the nonrelativistic scaling relation (1) with the scaling relation (2).

First, for any nuclear charges Z and $\tilde{Z}$ we can calculate the scaled charges Z' and $\tilde{Z}'$ from Eq. (2). Then, since the charges Z' and $\tilde{Z}'$ represent the corresponding nonrelativistic systems described by the TDSE, the nonrelativistic scaling (1) can be used to obtain the relations

$$\tilde{\lambda} = \lambda\left(\frac{Z'}{\tilde{Z}'}\right)^2; \quad \tilde{I} = I\left(\frac{\tilde{Z}'}{Z'}\right)^6 \tag{3}$$

between the wavelengths and peak intensities. Finally, the scaling relations (3) can be expressed through the true charges Z and $\tilde{Z}$ with the help of Eq. (2),

$$\tilde{\lambda} = \lambda\frac{1-\sqrt{1-Z^2/c^2}}{1-\sqrt{1-\tilde{Z}^2/c^2}};$$
$$\tilde{I} = I\left(\frac{1-\sqrt{1-\tilde{Z}^2/c^2}}{1-\sqrt{1-Z^2/c^2}}\right)^3. \tag{4}$$

If the scaling relations (4) are used for the laser parameters, the TDDE calculations for Z and $\tilde{Z}$ are expected to be in good agreement with each other. In the following, the method of solving the TDDE used in this paper is briefly introduced.

B. Method of solving the TDDE

The relativistic dynamics of the hydrogenlike ion in the laser field is described by the TDDE,

$$i\frac{\partial\Psi(t)}{\partial t} = H(t)\Psi(t), \tag{5}$$

where $\Psi(t)$ is the time-dependent wave function of the electron, and the total Hamiltonian $H(t)$ can be represented as a sum of two terms,

$$H(t) = H_0 + V(t). \tag{6}$$

Here H_0 is the time-independent field-free Dirac Hamiltonian,

$$H_0 = c(\boldsymbol{\alpha}\cdot\boldsymbol{p}) + c^2\beta + V_{\mathrm{C}}, \tag{7}$$

where $\boldsymbol{\alpha}$ and β are the Dirac matrices. We adopt the pointlike nucleus model, and thus the interaction V_{C} of the electron with the nucleus of the charge Z is described by the Coulomb potential:

$$V_{\mathrm{C}} = -\frac{Z}{r}. \tag{8}$$

The interaction with the external electromagnetic field $V(t)$ is represented within the dipole approximation,

$$V(t) = \boldsymbol{r}\cdot\boldsymbol{F}(t) = zF(t), \tag{9}$$

where $\boldsymbol{F}(t) = -d\boldsymbol{A}(t)/dt$ is the electric field strength, and $\boldsymbol{A}(t)$ is the vector potential. The field $\boldsymbol{F}(t)$ is assumed to be linearly polarized along the z axis. In this work, we make use of the ion-laser interaction term in the length gauge; earlier it was shown that the observables obtained by solving the TDDE in the length and velocity gauges coincide with each other if the numerical convergence is reached [10,14].

Our scheme to solve the TDDE generally follows the approach described in Ref. [10]. At the first step, we solve the time-independent Dirac equation for the unperturbed (field-free) hydrogenlike ion where the electron moves in the Coulomb potential of the nucleus only. The field-free eigenstates can be found by either direct expansion of the radial wave functions on a B-spline [26] basis set (see, for example, [27]) or with the help of the dual-kinetic-balance (DKB) approach [28]. Then the time-dependent Dirac wave function is expanded on the basis of the field-free eigenstates. The expansion coefficients can be found by employing various propagation schemes. For example, we consider the Crank-Nicolson propagation scheme [29], split-operator technique [30], and variable-order, variable-step Adams solver [31]. Below we give a more detailed description of the algorithm for solving the TDDE.

To solve Eq. (5), we expand the time-dependent Dirac wave function $\Psi(t)$ in a finite basis set which is represented by the eigenfunctions $\varphi_{n\kappa\mu}(\boldsymbol{r})$ of the field-free Hamiltonian,

$$\Psi(\boldsymbol{r},t) = \sum_{n,\kappa} C_{n\kappa\mu}(t)e^{-iE_{n\kappa}t}\varphi_{n\kappa\mu}(\boldsymbol{r}), \tag{10}$$

where $C_{n\kappa\mu}(t)$ are the expansion coefficients; the indices n,κ define the full set of basis states, n is the principal quantum number, κ is the angular momentum-parity quantum number, and μ is the projection of the total electron angular momentum on the z axis. The quantum number μ is conserved due to the axial symmetry along the z axis.

The angular momentum-parity quantum number κ is expressed through the orbital angular momentum l and total angular momentum j:

$$\kappa = (-1)^{l+j+1/2}(j+1/2). \tag{11}$$

The time-independent and orthonormal basis functions $\varphi_{n\kappa\mu}(\boldsymbol{r})$ are the eigenfunctions of the unperturbed Hamiltonian H_0:

$$H_0\varphi_{n\kappa\mu}(\boldsymbol{r}) = E_{n\kappa}\varphi_{n\kappa\mu}(\boldsymbol{r}), \tag{12}$$

$$\varphi_{n\kappa\mu}(\boldsymbol{r}) = \frac{1}{r}\begin{pmatrix} G_{n\kappa}(r)\Omega_{\kappa\mu}(\boldsymbol{n}) \\ iF_{n\kappa}(r)\Omega_{-\kappa\mu}(\boldsymbol{n})\end{pmatrix}, \quad \boldsymbol{n} = \frac{\boldsymbol{r}}{r}, \tag{13}$$

where $G_{n\kappa}(r)$ and $F_{n\kappa}(r)$ are the upper and lower radial components of the wave function $\varphi_{n\kappa\mu}(\boldsymbol{r})$ while $\Omega_{\kappa\mu}(\boldsymbol{n})$ is the spherical spinor. The radial components can be calculated numerically by solving ordinary differential equations. If B-spline expansions are straightforwardly used for this purpose (see, for example, Eq. (13) in Ref. [10] or Eq. (14) in Ref. [27]), then nonphysical (so-called spurious) states emerge among the solutions. To avoid such an undesirable effect, an appropriate modification of the B-spline basis set was suggested (the DKB approach [28]). For the hydrogenlike ions, however, it is easy to identify and remove the spurious states even if the DKB approach is not used. Therefore in our case we can use both DKB and non-DKB schemes and achieve the same results.

By substitution of the expansion (10) into the TDDE (5), the latter can be reduced to a set of first-order ordinary differential equations for the expansion coefficients,

$$i\frac{\partial}{\partial t}C_{K'}(t) = \sum_{K} V_{K'K}(t)C_K(t)e^{-i(E_K-E_{K'})t}, \tag{14}$$

where the indices K' and K represent the full sets of quantum numbers $\{n', \kappa', \mu\}$ and $\{n, \kappa, \mu\}$, respectively, and $V_{K'K}(t)$ is the time-dependent matrix element defined as

$$V_{K'K}(t) = \langle\varphi_{K'}|V(t)|\varphi_K\rangle. \tag{15}$$

In the length gauge, $V_{K'K}(t)$ may be written as

$$\begin{aligned} V_{K'K}(t) &= F(t)(-1)^{j'+j+\frac{1}{2}-\mu}\sqrt{(2j'+1)(2j+1)} \\ &\times \int_0^\infty dr\, r[G_{n'j'l'}(r)G_{njl}(r) + F_{n'j'l'}(r)F_{njl}(r)] \\ &\times \delta_{|l'-l|,1}\begin{pmatrix} j' & 1 & j \\ -\mu & 0 & \mu\end{pmatrix}\begin{pmatrix} j' & 1 & j \\ -\frac{1}{2} & 0 & \frac{1}{2}\end{pmatrix}. \end{aligned} \tag{16}$$

The radial integration in the matrix elements (16) is performed numerically using the Gauss-Legendre quadrature, and the $3j$-symbol analytical expressions are obtained for the angular integrals [32]. With the matrix elements $V_{K'K}(t)$ at hand, the time propagation in Eq. (14) is carried out numerically.

In all the calculations reported here, the ground $1s_{1/2}$ electron state is chosen as the initial state for the time propagation. The projection μ of the total electron angular momentum is equal to $1/2$. We choose the same B-spline basis set as in Ref. [10], with 500 B-splines of the 9th order. This number of B-splines provides sufficient number of the continuum (both positive and negative energy) as well as bound states for each angular momentum. The radial box size $R = (250/Z)$ a.u. is adopted, as was suggested in Ref. [10] and can be understood from Eq. (1).

The laser vector potential is chosen in the form of an N-cycle $\cos^2$-shaped pulse:

$$\boldsymbol{A}(t) = \begin{cases} \boldsymbol{e}_z A_0 \cos^2\left(\frac{\pi t}{T}\right)\sin(\omega t), & |t| < T/2, \\ 0, & |t| \geqslant T/2, \end{cases} \tag{17}$$

where ω is the photon energy, T is the pulse duration, $T = \frac{2\pi N}{\omega}$, and $A_0 = F_0/\omega$, F_0 is the peak electric field. We use the same laser pulse shape with a constant number of optical cycles $N = 20$ in all our calculations.

After the calculation of all the expansion coefficients $C_K(t)$ on the time grid, the ionization probability can be found as a projection of the final electron wave function onto the states φ_K with energies higher than mc^2:

$$\begin{aligned} P_{\rm ion} &= \sum_{\substack{K, \\ E_K \geqslant mc^2}} |\langle\Psi(t=T/2)|\varphi_K\rangle|^2 \\ &= \sum_{\substack{K, \\ E_K \geqslant mc^2}} |C_K(t=T/2)|^2. \end{aligned} \tag{18}$$

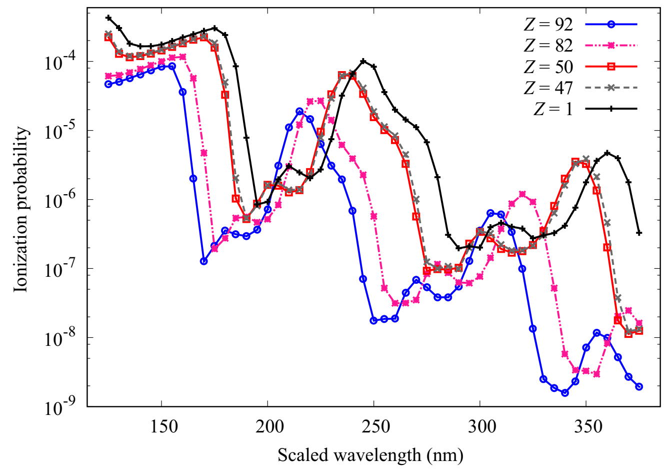

FIG. 1. Multiphoton ionization probability of the hydrogenlike ions with the nuclear charges Z (specified in the figure) as a function of the scaled carrier wavelength λZ^2. The laser pulse is $\cos^2$-shaped and contains 20 optical cycles at each scaled wavelength. The peak intensity is equal to 5×10^{22} W/cm^2 for $Z = 50$ and scaled according to Eq. (1) with Z^6 for the other nuclear charges.

III. RESULTS AND DISCUSSION

A. Scaling of the TDDE using the nonrelativistic scaling relations

First, we present the results of solving the TDDE for the hydrogenlike ions and laser pulse parameters after adopting the nonrelativistic scaling relations (1). Figure 1 shows the multiphoton ionization probabilities of several hydrogenlike ions. The field parameters are the same as in Ref. [10] for $Z = 50$ and properly scaled for the other nuclear charges. Our results for the ionization probability of the ion with the nuclear charge $Z = 50$ are in good agreement with those presented in Fig. 5 of Ref. [10].

Looking at the curves in Fig. 1, one can see that the nonrelativistic scaling does not work satisfactorily for the TDDE, while it is exact for the TDSE. The curve for $Z = 1$ essentially represents the nonrelativistic ionization probability because the relativistic effects are negligible for the hydrogen atom at the intensity and wavelengths used in the calculations (as tested by comparing the TDDE and TDSE results). Consequently, this curve also displays the ionization probabilities of the other hydrogenlike ions obtained by the nonrelativistic scaling. However, the curves corresponding to the higher nuclear charges and obtained by solving the TDDE are shifted from the curve for $Z = 1$. The shifts can be explained as relativistic effects that become significant for highly charged ions and increase with the nuclear charge Z. For a narrow range of Z numbers, the nonrelativistic scaling approximately works even for the TDDE (see, for example, the results for $Z = 47$ and $Z = 50$ in Fig. 1). However, for a wide Z range, the nonrelativistic scaling does not work even approximately.

B. Scaling of the TDDE by the new scaling relations

In Fig. 2, we show the multiphoton ionization probabilities of several hydrogenlike ions for the same laser pulse parameters at $Z = 50$ as in Fig. 1. However, for the other

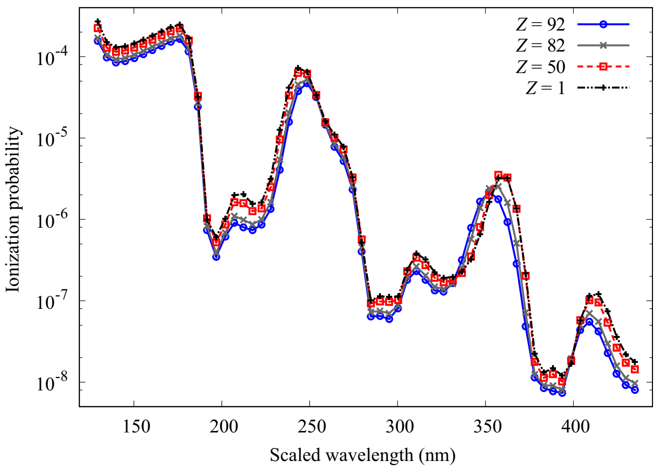

FIG. 2. Multiphoton ionization probability of the hydrogenlike ions with the nuclear charges Z (specified in the figure) as a function of the scaled carrier wavelength $\lambda Z'^2$. Z' is related to the true nuclear charge Z by Eq. (2). The laser pulse is $\cos^2$-shaped and contains 20 optical cycles at each scaled wavelength. The peak intensity is equal to 5×10^{22} W/cm^2 for $Z = 50$ and scaled according to Eq. (4) for the other nuclear charges.

nuclear charges the laser pulse parameters are calculated by the expressions (4). Compared with Fig. 1, we have also extended the wavelength range to include the five-photon ionization process.

The new scaling relations used in Fig. 2 take into account the dominant relativistic effect, the lowering of the ground-state energy level, that affects the multiphoton ionization process. Making use of these scaling laws allows us to nearly eliminate the shifts of the ionization curves in Fig. 1. Looking at Figs. 1 and 2, one can notice that the correction of the (ground-state) ionization potential with the help of Eq. (4) can change the ionization probabilities by orders of magnitude at some wavelengths (near the ionization thresholds). Therefore the combined scaling relations suggested in our work can be very useful for accurate predictions of the ionization dynamics of the hydrogenlike ions in a wide range of nuclear charges. The four curves in Fig. 2 are quite close to each other, but small discrepancies still exist. These deviations are caused by other relativistic effects not taken into account in Eq. (4).

C. Intensity scaling

In this section, we consider the scaling properties of the multiphoton ionization in a wide range of laser peak intensities. We have calculated the multiphoton ionization probability as a function of the nuclear charge Z for five fixed peak intensities of the laser pulse (17). For $Z = 50$, we use the peak intensities of 5×10^{22}, 1×10^{23}, 5×10^{23}, 1×10^{24},

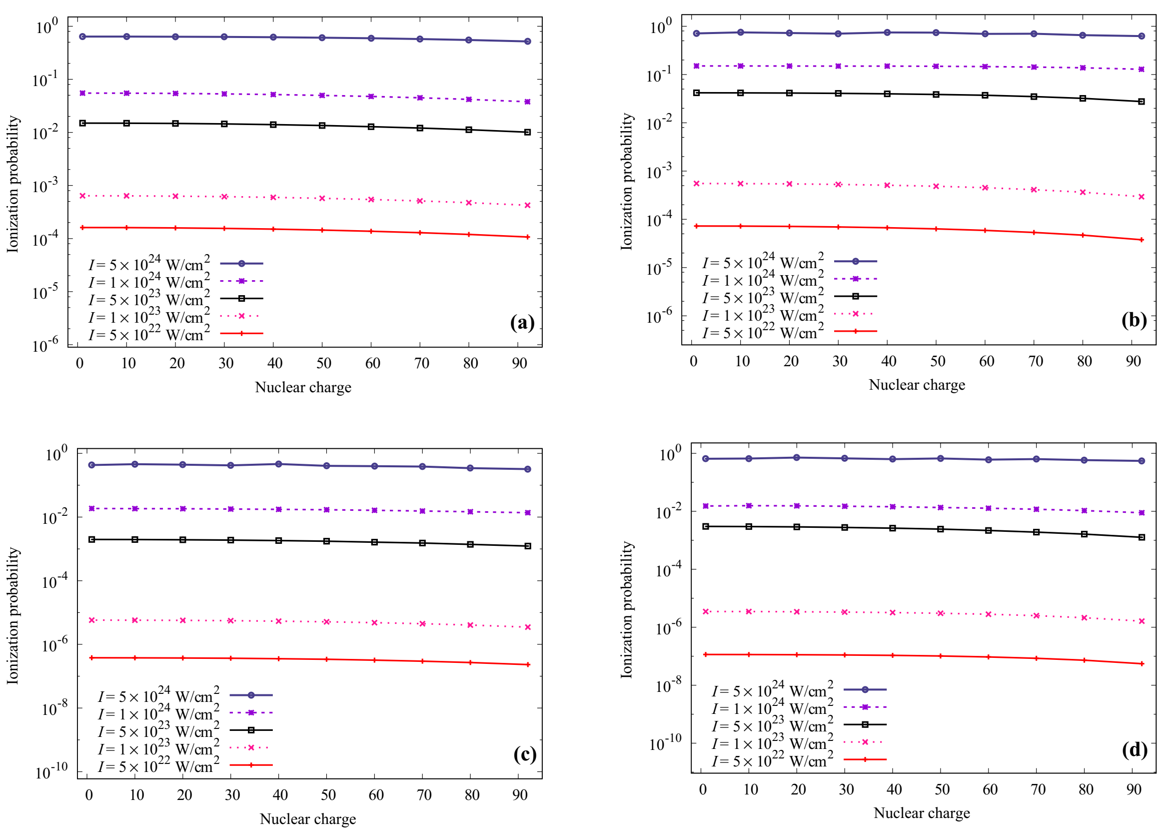

FIG. 3. Multiphoton ionization probability of the hydrogenlike ions as a function of the nuclear charge Z. (a) Two-photon ionization process with a laser wavelength of 0.06 nm for $Z = 50$. (b) Three-photon ionization process with a laser wavelength of 0.094 nm for $Z = 50$. (c) Four-photon ionization process with a laser wavelength of 0.12 nm for $Z = 50$. (d) Five-photon ionization process with a laser wavelength of 0.158 nm for $Z = 50$. In all subfigures, for $Z = 50$, the peak intensity range is 5×10^{22} to 5×10^{24} W/cm^2. For the other ions, the laser peak intensity and wavelength are scaled according to Eq. (4).

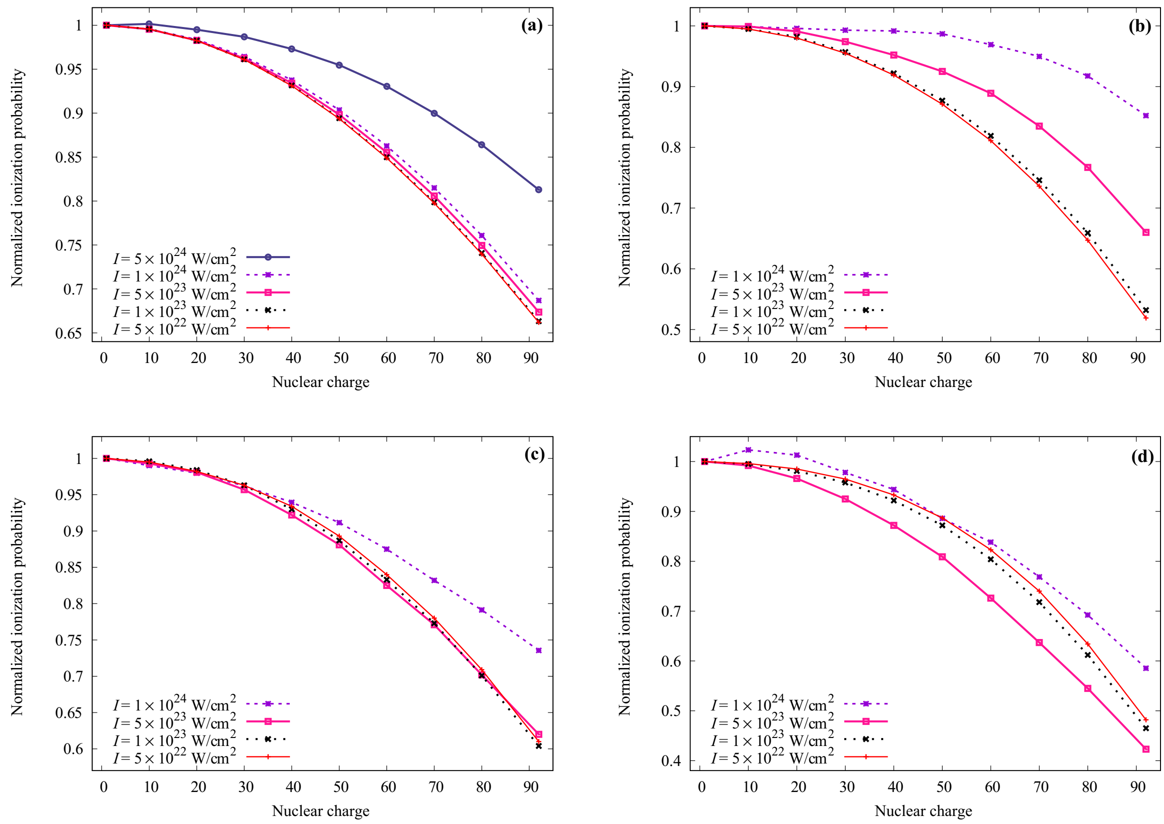

FIG. 4. Ionization probabilities of the hydrogenlike ions normalized to unity at $Z = 1$. (a) For $Z = 50$, the wavelength is 0.06 nm (two-photon ionization), and the peak intensity range is 5×10^{22} to 5×10^{24} W/cm^2. (b) For $Z = 50$, the wavelength is 0.094 nm (three-photon ionization), and the peak intensity range is 5×10^{22} to 1×10^{24} W/cm^2. (c) For $Z = 50$, the wavelength is 0.12 nm (four-photon ionization), and the peak intensity range is 5×10^{22} to 1×10^{24} W/cm^2. (d) For $Z = 50$, the wavelength is 0.158 nm (five-photon ionization), and the peak intensity range is 5×10^{22} to 1×10^{24} W/cm^2. In all subfigures, for the other ions, the laser peak intensity and wavelength are scaled according to Eq. (4).

and 5×10^{24} W/cm^2. For the other nuclear charges, the peak intensities are scaled as suggested by expression (4). Two-, three-, four-, and five-photon ionization processes have been investigated (see Fig. 3). Here, we study nonresonant ionization, so the wavelengths have been chosen accordingly to avoid situations where the resonantly enhanced multiphoton ionization (REMPI) can take place.

In Fig. 3 one can see that the ionization probability is almost independent of the nuclear charge Z for the range of intensities and multiphoton processes (from two-photon to five-photon ionization) under consideration, if plotted on a logarithmic scale. Indeed, for light ions the ionization probability is Z independent even on the linear scale. The results presented in Fig. 3 cover a wide range of nuclear charges, laser wavelengths, and pulse peak intensities. We can thus conclude that the scaling relations (4) are quite accurate and properly account for the dominant relativistic effect in multiphoton ionization. In Sec. III D the remaining relativistic effects, especially for heavy ions, are discussed that cause the remaining deviations of the curves in Fig. 3 from straight horizontal lines.

D. Relativistic effects

In the relativistic ionization regime discussed in the previous section, the ionization probabilities of the highly charged ions differ only slightly from the ionization probabilities of the hydrogen atom, if the laser pulse parameters are scaled using the new scaling laws (4). The remaining small deviations of the curves in Fig. 3 from the straight horizontal lines can be attributed to smaller relativistic effects not reflected in Eq. (4).

To further examine these small relativistic effects, we discuss here the ionization probabilities normalized to unity at $Z = 1$. Displayed on a linear probability scale in Fig. 4 are the same processes of two-, three-, four-, and five-photon ionization as shown on a logarithmic scale in Fig. 3. Two conclusions can be made when looking at Fig. 4. First, for each peak intensity, the normalized ionization probability decreases with increasing nuclear charge Z. That means the scaling relations (4) overestimate the ionization probability of highly charged ions, and this effect becomes larger for larger Z. This is not surprising, since it is expected that any relativistic effects are more pronounced for heavier ions. In the range of the wavelengths and peak intensities used in the calculations, the dependence of the normalized probability on Z is approximately quadratic. At the highest intensity $I = 5 \times 10^{24}$ W/cm^2, the saturation of the ionization is reached in the three-, four-, and five-photon ionization processes for most of the Z values used in the calculations [not shown in Figs. 4(b), 4(c) and 4(d)] and the quadratic dependence on Z of the remaining relativistic effects breaks down. The saturation effects are visible even at the lower intensity $I = 1 \times 10^{24}$ W/cm^2 in Figs. 4(b) and 4(d).

The second conclusion concerns the dependence of the normalized ionization probability on the peak intensity of the laser pulse when the saturation is not yet reached. Multiphoton ionization is an extremely nonlinear process, and its dependence on the intensity at each value of Z can be nonmonotonous and very complex, as one can see in Figs. 4(c) and 4(d).

The normalized ionization probabilities presented in Fig. 4 can help to isolate the small remaining relativistic effects, which still show up after compensation of the main relativistic effect due to the shift of the ionization potential by the scaling laws (4). For the multiphoton ionization processes studied here, the relativistic effects can be easily quantified and do not exceed 40% of the nonrelativistic probabilities for the hydrogen atom (see Fig. 4). Such effects as, e.g., spin-orbit coupling, are quite small compared to the main relativistic effect, where the latter can cause a change of the ionization probabilities for up to four orders of magnitude even at the lowest intensity $I = 5 \times 10^{22}$ W/cm^2 used in the calculations (for example, compare the data for $Z = 92$ in Figs. 1 and 2).

IV. CONCLUSION

In this paper, approximate scaling relations with respect to the nuclear charge have been presented for the TDDE describing hydrogenlike ions subject to laser fields within the dipole approximation. As a case study, the scaling relations (4) have been applied to the multiphoton ionization yields of hydrogenlike ions with various nuclear charges in the two- to five-photon regime. The ion yields were calculated by solving the TDDE and the results obtained for different wavelengths and laser peak intensities, both scaled accordingly. While the previously derived nonrelativistic scaling relations are found to be clearly insufficient in the relativistic regime described by the TDDE, the new scaling relations lead to good agreement between the ionization probabilities of the hydrogenlike ions with different nuclear charges. Note that depending on the nuclear charge and laser parameters, the new scaling factors modify not only the unscaled ion yields, but also the ones scaled by the nonrelativistic scaling factor by several orders of magnitude and are thus very important even for order-of-magnitude estimates.

Also, the dependence of the multiphoton ionization yields on the nuclear charge Z for a wide range of laser peak intensities has been investigated. It was found that the nonresonant two-, three-, four-, and five-photon ionization probabilities are almost Z independent, if the laser parameters are scaled by the scaling laws (4) introduced in this work. This uniform behavior of the properly scaled results that covers a wide range of nuclear charges, laser wavelengths, and intensities is expected to be very useful for the planning and analysis of future experiments. Furthermore, the scaling relations may allow for a simple estimate of ion yields in laser fields of very high intensities, as they may be needed in corresponding laser-field-induced plasma simulations or for considering possible radiation damage.

The remaining small deviations of the scaled solutions of the TDDE reveal, on the other hand, the existence of further relativistic effects that are neither reflected in the nonrelativistic scaling relations (as they are exact) nor in the relativistic shift of the ionization potential. Away from saturation, these small relativistic effects not captured by the scaling relations proposed in this work are found to show an almost quadratic dependence on the nuclear charge.

Finally, hydrogenlike ions with variable charge may be used as a tool for laser-pulse characterization or calibration, especially for light sources with extreme peak intensities. If the scaling relations are valid, the ion yield obtained with a laser pulse of, e.g., unknown laser peak intensity may be compared to the properly scaled ion yield obtained for an ion with lower nuclear charge exposed to a well-characterized laser pulse of lower intensity. On the other hand, such comparisons could be used to uniquely identify experimentally beyond-dipole or other relativistic effects not yet contained in the scaling relations. This would be helpful for guiding subsequent theoretical studies.

ACKNOWLEDGMENTS

This work was supported by the RFBR (Grant No. 16-02-00233) and by the SPbSU-DFG (Grants No. 11.65.41.2017 and No. STO 346/5-1). I.V.I. acknowledges support from the FAIR-Russia Research Center and the German-Russian Interdisciplinary Science Center (G-RISC) funded by the German Federal Foreign Office via the German Academic Exchange Service (DAAD). A.S. and I.V.I. acknowledge financial support by the German Ministry of Education and Research (BMBF) within the APPA R&D (Grants No. 05P15KHFAA and No. 05P18KHFAA).

[1] J.-P. Chambaret, O. Chekhlov, G. Cheriaux, J. Collier, R. Dabu, P. Dombi, A. M. Dunne, K. Ertel, P. Georges, J. Hebling *et al.*, Proc. SPIE **7721**, 77211D (2010).

[2] G. A. Mourou, G. Korn, W. Sandner, and J. L. Collier (eds.), *ELI-Extreme Light Infrastructure Science and Technology with Ultra-Intense Lasers WHITEBOOK* (THOSS Media GmbH, Berlin, 2011).

[3] T. Tschentscher and R. Feidenhans'l, Synchrotron Radiat. News **30**, 21 (2017).

[4] M. Dunne and B. Schoenlein, Synchrotron Radiat. News **30**, 7 (2017).

[5] M. Vogel, W. Quint, G. G. Paulus, and Th. Stöhlker, Nucl. Instrum. Methods B **285**, 65 (2012).

[6] S. Ringleb, M. Vogel, S. Kumar, W. Quint, G. G. Paulus, and Th. Stöhlker, Phys. Scr. **T166**, 014067 (2015).

[7] S. Selstø, E. Lindroth, and J. Bengtsson, Phys. Rev. A **79**, 043418 (2009).

[8] M. S. Pindzola, J. A. Ludlow, and J. Colgan, Phys. Rev. A **81**, 063431 (2010).

[9] M. S. Pindzola, Sh. A. Abdel-Naby, F. Robicheaux, and J. Colgan, Phys. Rev. A **85**, 032701 (2012).

[10] Y. V. Vanne and A. Saenz, Phys. Rev. A **85**, 033411 (2012).

[11] E. B. Rozenbaum, D. A. Glazov, V. M. Shabaev, K. E. Sosnova, and D. A. Telnov, Phys. Rev. A **89**, 012514 (2014).

[12] M. Klaiber and K. Z. Hatsagortsyan, Phys. Rev. A **90**, 063416 (2014).

[13] M. Klaiber, E. Yakaboylu, C. Müller, H. Bauke, G. G. Paulus, and K. Z. Hatsagortsyan, J. Phys. B: At., Mol. Opt. Phys. **47**, 065603 (2014).

[14] I. V. Ivanova, A. I. Bondarev, I. A. Maltsev, D. A. Tumakov, and V. M. Shabaev, J. Phys.: Conf. Ser. **635**, 092040 (2015).

[15] A. S. Simonsen, T. Kjellsson, M. Førre, E. Lindroth, and S. Selstø, Phys. Rev. A **93**, 053411 (2016).

[16] I. V. Ivanova, A. Saenz, A. I. Bondarev, I. A. Maltsev, V. M. Shabaev, and D. A. Telnov, J. Phys.: Conf. Ser. **875**, 022031 (2017).

[17] T. Kjellsson, S. Selstø, and E. Lindroth, Phys. Rev. A **95**, 043403 (2017).

[18] T. Kjellsson, M. Førre, A. S. Simonsen, S. Selstø, and E. Lindroth, Phys. Rev. A **96**, 023426 (2017).

[19] D. A. Telnov, D. A. Krapivin, J. Heslar, and S.-I. Chu, J. Phys. Chem. A **122**, 8026 (2018).

[20] P. Lambropoulos and X. Tang, J. Opt. Soc. Am. B **4**, 821 (1987).

[21] L. B. Madsen and P. Lambropoulos, Phys. Rev. A **59**, 4574 (1999).

[22] A. S. Alnaser, X. M. Tong, T. Osipov, S. Voss, C. M. Maharjan, B. Shan, Z. Chang, and C. L. Cocke, Phys. Rev. A **70**, 023413 (2004).

[23] M. G. Pullen, W. C. Wallace, D. E. Laban, A. J. Palmer, G. F. Hanne, A. N. Grum-Grzhimailo, K. Bartschat, I. Ivanov, A. Kheifets, D. Wells, H. M. Quiney, X. M. Tong, I. V. Litvinyuk, R. T. Sang, and D. Kielpinski, Phys. Rev. A **87**, 053411 (2013).

[24] S.-F. Zhao, A.-T. Le, C. Jin, X. Wang, and C. D. Lin, Phys. Rev. A **93**, 023413 (2016).

[25] W. C. Wallace, O. Ghafur, C. Khurmi, S. Sainadh U, J. E. Calvert, D. E. Laban, M. G. Pullen, K. Bartschat, A. N. Grum-Grzhimailo, D. Wells, H. M. Quiney, X. M. Tong, I. V. Litvinyuk, R. T. Sang, and D. Kielpinski, Phys. Rev. Lett. **117**, 053001 (2016).

[26] C. de Boor, *A Practical Guide to Splines*, Applied Mathematical Sciences, revised edition (Springer-Verlag, New York, 2001), Vol. 27.

[27] W. R. Johnson, S. A. Blundell, and J. Sapirstein, Phys. Rev. A **37**, 307 (1988).

[28] V. M. Shabaev, I. I. Tupitsyn, V. A. Yerokhin, G. Plunien, and G. Soff, Phys. Rev. Lett. **93**, 130405 (2004).

[29] J. Crank and P. Nicolson, Proc. Cambridge Philos. Soc. **43**, 50 (1947).

[30] J. A. Fleck, J. R. Morris, and M. D. Feit, Appl. Phys. **10**, 129 (1976).

[31] W. H. Press, S. A. Teukolsky, W. T. Vetterling, and B. P. Flannery, *Numerical Recipes in Fortran 77*, 2nd ed., Fortran Numerical Recipes Vol. 1 (Cambridge University Press, Cambridge, 1992).

[32] D. A. Varshalovich, A. N. Moskalev, and V. K. Khersonskii, *Quantum Theory of Angular Momentum* (World Scientific, Singapore, 1988).